Korean J. Chem. Eng., 33(11), 3109-3114 (2016)
DOI: 10.1007/s11814-016-0175-6

pISSN: 0256-1115
eISSN: 1975-7220

Kinetic modeling and dynamic simulation for the catalytic wet air oxidation of aqueous ammonia to molecular nitrogen

Deuk Ki Lee*,†, Jeong Shik Cho*, Taejong Yu*, Yong Su Lee, Jae Wan Choe**, and Sang Soo Lee****

*Department of Fire Safety, Gwangju University, Gwangju 61743, Korea
**Department of Civil Engineering, Gwangju University, Gwangju 61743, Korea
(*Received 20 March 2016 • accepted 20 June 2016*)

Abstract−A kinetic model for the catalytic wet air oxidation of aqueous ammonia over Ru/TiO_2 catalyst was developed considering the consecutive reaction steps as follows: (i) formation of active oxygen sites O* by the dissociative adsorption of aqueous O_2 on the catalyst, (ii) oxidation of aqueous NH_3 by the reaction with three O* sites to produce HNO_2, (iii) aqueous phase dissociation of HNO_2 into H^+ and NO_2^-, (iv) formation of NH_4^+ by the association of NH_3 with the HNO_2-dissociated H^+, (v) formation of N_2 by the aqueous phase reaction between NO_2^- and NH_4^+, (vi) formation of NO_3 by the reaction of NO_2^- with an O* site. For each reaction step, a rate equation was derived and its kinetic parameters were optimized by experimental data fitting. Activation energies for the reactions (ii), (v), and (vi) were 123.1, 76.7, and 54.5 kJ/mol, respectively, suggesting that the oxidation reaction of aqueous NH_3 to HNO_2 was a rate-determining step. From the simulation using the kinetic parameters determined, the initial pH adjustment of the ammonia solution proved to be critical for determining the oxidation product selectivity between desirable N_2 and undesirable NO_3^- as well as the degree of oxidation conversion of ammonia.

Keywords: Catalytic Wet Air Oxidation, Aqueous Ammonia, Kinetics, Modeling, Activation Energy, pH

INTRODUCTION

Aqueous ammonia in wastewaters is of environmental concern due to its detrimental impact on natural water resources, such as surface water eutrophication and ground water contamination by nitrates formed eventually. As an efficient and environment-friendly technology applicable to the removal of ammonia from various industrial wastewaters of generally high toxicity, catalytic wet air oxidation of ammonia by which pollutant ammonia can be removable mainly to molecular nitrogen has been of interest. As reviewed by Oliviero et al. [1], the supported catalysts of precious metals or base metals are basically required for higher oxidation conversion of ammonia at a reaction condition of less severity. It is most important in this technology that ammonia should be oxidized selectively to N_2 instead of the formation of hazardous nitrates as final products. Therefore, most research efforts have been so far focused on the development of the oxidation reaction active and simultaneously N_2-selective catalyst [1-11]. Generally, noble metal catalysts are more active and selective for ammonia conversion and for N_2 formation, respectively, than transition metal catalysts like Ni and Mn [2,3]. On the reaction performance of the noble metal catalysts of Pt, Pd, and Ru, the Pt was the most active in the aqueous ammonia oxidation [3,4,10,12], and the Pd catalyst turned to be the most selective toward N_2 [10,12]. Lousteau et al. [10] proposed that the oxygen coverage at the catalyst surface should not be too high to promote the N-N recombination leading to N_2, and therefore the catalyst with intermediate value of metal oxygen bond energy should be preferred to optimize both the activity and the selectivity toward N_2. This can be a reason why noble metals exhibit better performance than transition metals in the catalytic wet oxidation of aqueous ammonia. They suggested the reaction between an adsorbed nitrous acid species (HNO_2*) and an adsorbed oxygen atom (O*) to produce nitric acid, which in turn decomposed into nitrates and a proton. Their proposal basically supports that the selective formation of N_2 against NO_3^- belongs to a heterogeneous reaction depending on a kind of catalytic function. However, the homogeneous reaction between ammonium and nitrite ions in water was also admitted in their study as a route of N_2 formation. Despite such research efforts ve, it is still difficult to reach a consensus on the roles of catalyst and the governing reaction mechanism in the catalytic wet air oxidation reaction of ammonia.

In previous studies [13,14] for the catalytic wet air oxidation of ammonia over Ru/TiO_2, the catalyst was proposed to be responsible only for the oxidation of aqueous ammonia, producing a molecule of nitrous acid. It was also reported that the preferential production of N_2 was due to the homogeneous aqueous phase reaction of the nitrous acid-dissociated NO_2^- with NH_4^+ ions, which would be kinetically more rapid than the reaction of NO_2^- with O* forming NO_3^-. For greater understanding about the proposed reaction mechanism in the catalytic wet air oxidation of ammonia, information on the kinetics of each constituting reaction step would be helpful. In this regard, the current study is aimed at the development of a kinetic model for the catalytic wet air oxidation of aqueous ammonia over the Ru/TiO_2 catalyst on the basis of the

†To whom correspondence should be addressed.
E-mail: dklee@gwangju.ac.kr
‡This article is dedicated to Prof. Seong Ihl Woo on the occasion of his retirement from KAIST.

reaction mechanism proposed and the experimental data obtained before [13,14]. Throughout the simulation for the reaction using the kinetic data obtained, the effects of the initial pH of the ammonia solution on the reaction performance such as ammonia conversion, N_2 yield, and NO_3^- formation has been discussed.

KINETIC DATA AND MODELING

1. Experimental Data

The kinetic data used in the current study for modeling the catalytic wet oxidation of ammonia were obtained from previous experiments [13]. The catalyst was TiO_2-supported Ru (3 wt%), and the reaction experiments for aqueous ammonia solution of initial concentration 1,000 ppm (58.82×10^{-3} mol L^{-1}) with initially adjusted pH_i, 12.2-12.4, at 25 °C were conducted in a batch reactor under the gas phase oxygen pressures (P_{O_2}), 4.8-11.1 bar, at reaction temperatures, 160-220 °C. More experimental details can be found elsewhere [13].

2. Derivation of Kinetics

The reaction mechanism for the catalytic wet air oxidation of ammonia previously proposed [13,14] is summarized in Table 1. From the O_2 activation step, catalyst surface coverage of the activated oxygen, [O*], is obtained as follows:

$$[O^*]=\frac{\sqrt{K_1P_{O_2}}}{1+\sqrt{K_1P_{O_2}}}, \tag{1}$$

where, K_1 (bar^{-1}) is the dissociative adsorption equilibrium constant for O_2, P_{O_2} (bar) is the partial pressure of O_2 in the gas phase of the reactor. For the reactions R2-R6, the rate equations are represented as follows:

$$r_2=k_2[NH_3][O^*]^3, \tag{2}$$

$$r_3=k_3([HNO_2]-[NO_2^-][H^+]/K_3), \tag{3}$$

$$r_4=k_4([NH_4^+]-[NH_3][H^+]/K_4), \tag{4}$$

$$r_5=k_5[NO_2^-][NH_4^+], \tag{5}$$

$$r_6=k_6[NO_2^-][O^*], \tag{6}$$

where, k_j (j=2-6) are the reaction rate constants, and the species in brackets represent the concentrations (mol L^{-1}) in the aqueous phase. Acid dissociation constants, K_3 and K_4 at a reaction temperature T (°C) are computed by using the Clasius-Clapeyron equation as follows [15]:

Table 1. Reaction mechanism for the catalytic wet oxidation of ammonia

O_2 activation	$O_2+2^* \overset{K_1}{\Leftrightarrow} 2O^*$	R1
HNO_2 formation	$NH_3+3O^* \xrightarrow{k_2} HNO_2+H_2O+3^*$	R2
NO_2^- formation	$HNO_2 \overset{K_3}{\Leftrightarrow} H^+ + NO_2^-$, pK_{HNO_2}=3.35 at 25 °C	R3
NH_4^+ formation	$NH_4^+ \overset{K_4}{\Leftrightarrow} NH_3+H^+$, $pK_{NH_4^+}$=9.25 at 25 °C	R4
N_2 formation	$NO_2^-+NH_4^+ \xrightarrow{k_5} N_2+2H_2O$	R5
NO_3^- formation	$NO_2^-+O^* \xrightarrow{k_6} NO_3^-+^*$	R6

$$K_3=10^{-3.35}\exp\left\{\frac{14.6\times10^3}{R}\left(\frac{1}{298}-\frac{1}{T+273}\right)\right\}, \tag{7}$$

$$K_4=10^{-9.25}\exp\left\{\frac{52.21\times10^3}{R}\left(\frac{1}{298}-\frac{1}{T+273}\right)\right\}, \tag{8}$$

where, R is the gas constant, 8.314 J mol^{-1} K^{-1}. A kinetic equation for each component is given as follows:

$$\frac{d[NH_3]}{dt}=r_4-r_2, \tag{9}$$

$$\frac{d[NH_4^+]}{dt}=-r_4-r_5, \tag{10}$$

$$\frac{d[HNO_2]}{dt}=r_2-r_3, \tag{11}$$

$$\frac{d[NO_2^-]}{dt}=r_3-r_5-r_6, \tag{12}$$

$$\frac{d[N_2]}{dt}=r_5, \tag{13}$$

$$\frac{d[NO_3^-]}{dt}=r_6, \tag{14}$$

3. Solution pH Calculation

As the oxidation reaction over the catalyst proceeds, one mole of NH_3 oxidation leads to one mole of HNO_2 production by the reaction R2. Nitrite ions dissociated from the HNO_2 can be converted to N_2 or NO_3^- by reaction R5 or R6, respectively. The molar number of nitrites converted to N_2 and NO_3^- can be calculated from the yields of N_2 and NO_3^- produced. Protons from the HNO_2 dissociation are responsible for the decrease in the solution pH, but parts of them, being used to transform aqueous NH_3 to NH_4^+ via the reaction R4, have no effect on the pH. Because a half molar amount of N_2 formed results from NH_4^+, net molar number of protons affecting the pH of the resultant solution can be calculated as follows [13,14]:

$$\text{mol } H^+_{net}=\text{mol } NO_2^- +(\text{mol } N_2)/2+\text{mol } NO_3^-, \tag{15}$$

Therefore, for the solution of volume 100 mL, pH or pOH evaluated at 25 °C is given by

$$pH_{25} \text{ or } pOH_{25}=-\log\left(\frac{|\text{mol } H^+_{net}-\text{mol } OH^-_{25,i}|}{0.1}\right), \tag{16}$$

where, mol $OH^-_{25,i}$ indicates the molar number of hydroxide ions present initially in the feed solution at 25 °C after the pH adjustment to 12.2. Further details in the solution pH calculation can be found elsewhere [13,14].

The term $[H^+]$ used in the kinetic Eqs. (3) and (4) represents the molar concentration of hydronium ions for the reacting solution at a reaction temperature T. This can be calculated by

$$[H^+]=10^{-pH_T}, \tag{17}$$

where, pH_T is the solution pH at reaction temperature T (°C), and can be calculated as

$$pH_T \text{ or } pOH_T=-\log\left(\frac{|\text{mol } H^+_{net}-\text{mol } OH^-_{T,i}|}{0.1}\right), \tag{18}$$

where, mol $OH^-_{T,i}$ indicates the molar number of hydroxide ions present when the temperature of the feed solution of the initial pH 12.2 at 25 °C is raised to the reaction temperature, T. It can be calculated by using the following relationship:

$$pH_{T,i}=pH_{25,i}\left\{1-\left(\frac{pK_{W,25}-pK_{W,T}}{pK_{W,25}}\right)\right\}, \quad (19)$$

where, $pK_{W,25}=pH_{25}+pOH_{25}=14$, and $pK_{W,T}$ is given by the following [16]:

$$pK_{W,T}=5\times10^{-5}(T+273)^2-0.0518(T+273)+24.605, \quad (20)$$

For example, $pK_{W,200}=11.3$ at 200 °C. The $pH_i=12.2$ at 25 °C corresponds to the $pH_i=9.85$ at 200 °C by Eq. (19). The initial molar number of hydroxyl ions in the 100 mL solution of $pH_i=12.2$ at 25 °C is calculated by mol $OH^-_{25,i}=10^{-(14+12.2)}10^{-1}=1.58\times10^{-3}$ mol, which can be used in Eq. (16). If the solution temperature is raised from 25 to 200 °C without any oxidation reaction, the initial molar number is calculated by mol $OH^-_{200,i}=10^{-(11.3+9.85)}10^{-1}=3.55\times10^{-3}$ mol, which can be used in Eq. (18).

4. Kinetic Parameter Estimation

With initial trial values for the equilibrium constants K_1 and the rate constants k_2-k_6, Eqs. (9)-(14) were integrated using the Matlab function, ode23t. The predicted results were compared with the experimental data at a specified reaction condition, and the optimum constant values were estimated using the Matlab function, fminsearch, by minimizing the following objective function:

$$F_{min}=\left(\frac{X_{NH_3-N,p}-X_{NH_3-N,e}}{X_{NH_3-N,e}}\right)^2+\left(\frac{Y_{N_2,p}-Y_{N_2,e}}{Y_{N_2,e}}\right)^2+\left(\frac{C_{NO_3,p}-C_{NO_3,e}}{C_{NO_3,e}}\right)^2, \quad (21)$$

where, X_{NH_3-N} is the conversion of NH_3-N, Y_{N_2} is the N_2 yield, C_{NO_3} is the concentration of NO_3^- in ppm at a reaction time, and the subscripts p and e denote the values predicted and experimented, respectively. Because the nitrogen balances in the experiments mostly did not meet 100% as reported previously [13], the NO_2-N concentration, of which value was the lowest among the reaction products, was not reflected in the objective function.

RESULTS AND DISCUSSION

Fig. 1 shows the kinetic model predictions in comparison with the experimental results at T=200 °C under $P_{O_2}=7.9$ bar for the 1,000 ppm NH_3 solution of $pH_i=12.2$. Experimental data of NH_3-N conversion, N_2 yield, and NO_3^- concentration, as shown in Fig. 1(a) and (b), are well represented by the kinetic model with the optimally determined constant values ($K_1=3.700\times10^{-3}$ bar^{-1}, $k_2=2.414\times10^{2}$ h^{-1}, $k_3=2.126\times10^{7}$ h^{-1}, $k_4=6.270\times10^{-2}$ h^{-1}, $k_5=1.763\times10^{4}$ L mol^{-1} h^{-1}, $k_6=3.016\times10^{1}$ h^{-1}) using Eq. (21). Kinetic model prediction of NO_2-N concentration deviates from the experimental data at earlier stage of the reaction, as shown in Fig. 1(c). However, its overall profile looks successful in suggesting the role of NO_2^- species as the oxidation reaction intermediates for the final products, N_2 and NO_3^-. Fig. 1(d) shows the model predictions of the solution pH evaluated at 25 °C (pH_{25}) and the reacting solution pH at temperature 200 °C (pH_{200}). The profile of the predicted

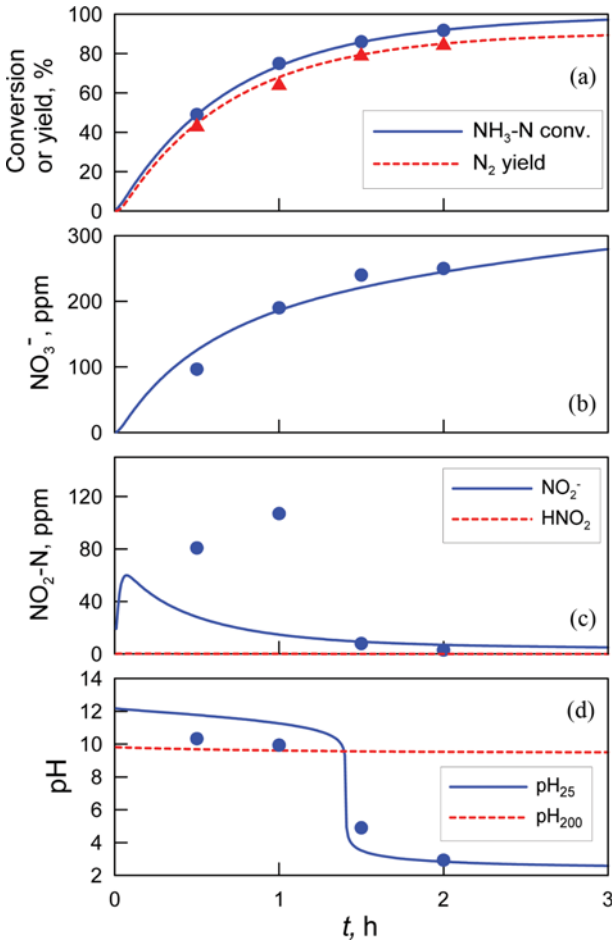

Fig. 1. Kinetic model predicted profiles based on the optimally determined equilibrium and rate constant values in comparison with the experimental results ((a) NH_3-N conversion and N_2 yield, (b) NO_3^- concentration, (c) NO_2-N concentration, and (d) pH_{25}) for the ammonia solution of $pH_{25,i}=12.2$ at T=200 °C under $P_{O_2}=7.9$ bar.

pH_{25} is consistent with pH data of the solution measured at 25 °C, specifying an equivalence point at the NH_3-N conversion of about 84.2%. However, no equivalence point exists on the pH_{200} irrespective of the conversion up to near 100%. This indicates that the amount of hydroxyl ions present initially in the ammonia solution at the reaction temperature 200 °C is much more than that of the protons produced by the oxidation conversion, and that the reaction at 200 °C has proceeded in the solution under alkaline condition.

Fig. 2 shows the Arrhenius plot for the equilibrium and rate constants, which were determined from such data fitting as above at different reaction temperatures, 160, 180, 200 and 220 °C. Being linearly plotted, each kinetic constant can be represented by the Arrhenius equation. For the aqueous phase reaction R4, because the backward reaction takes place to form NH_4^+ from initially predominant aqueous NH_3 in the reactant solution of $pH_i=12.2$, the backward reaction rate constant (k_{-4}) should be considered. It can be computed using the relation, $k_{-4}=k_4/K_4$, for instance, $k_{-4}=4.584\times10^{4}$ at 200 °C. Among the aqueous phase reactions, the HNO_2 dissociation reaction (R2) is the fastest. Therefore, NO_2^- is always

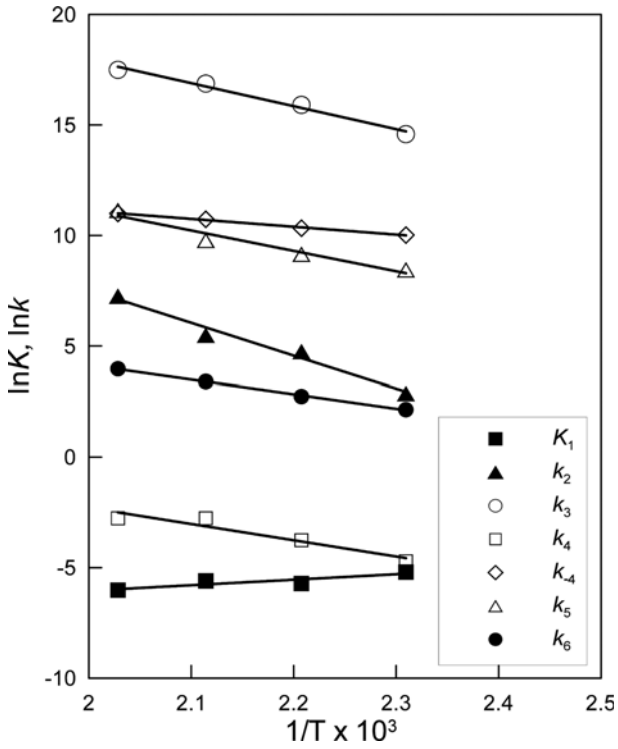

Fig. 2. Arrhenius plot for the equilibrium and rate constants for the reactions in Table 1.

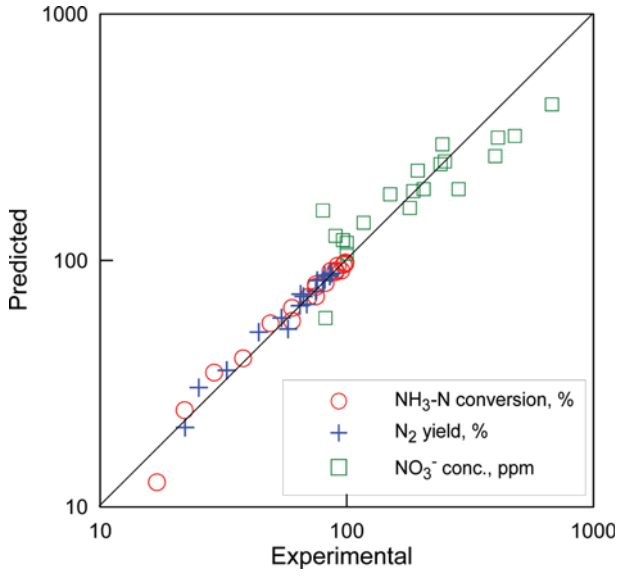

Fig. 3. Parity plots for NH_3-N conversion, N_2 yield, and NO_3^- concentration where the predicted data are based on the parameter values in Table 2 for the oxidation reaction of the 1,000 ppm NH_3 solution of $pH_{25,i}$=12.2.

available in the solution for the N_2-formation reaction (R5) once HNO_2 is produced by the oxidation reaction (R2) under alkaline water condition. The kinetic rate of the reverse R4 is fast enough to make NH_4^+ for the R5 as long as the reaction temperature is not higher than 220 °C. The rate constants, as shown in Fig. 2, suggest that all the homogeneous aqueous phase reactions of R3, the reverse R4, and R5 are kinetically faster than the heterogeneous catalytic reactions of R2 and R6 at all temperatures. Particularly, much higher values of k_5 as compared to those of k_6 confirms the intuition in the previous paper [14] that the homogeneous aqueous phase N_2-forming reaction (R5) of the nitrous acid-dissociated NO_2^- with NH_4^+ ions would be kinetically more rapid than the catalytic reaction (R6) of NO_2^- with O* forming NO_3^-.

The values of the enthalpy of dissociative adsorption of O_2 and activation energies as well as those of pre-exponential factors for the kinetic constants are listed in Table 2. First, the dissociative adsorption of O_2 onto the Ru/TiO_2 catalyst (R1) is estimated to be a mild-exothermic process with the enthalpy of adsorption of −20.7 kJ/mol. Activation energy in the ammonia oxidation reaction (R2) is estimated to be 123.1 kJ/mol. This is close to the apparent activation energy, 104 kJ/mol, obtained under the assumption that the ammonia conversion follows the first-order kinetics with respect to the ammonia concentration, as reported in the previous paper [13]. Activation energies in the reactions for N_2 and NO_3^- formation are estimated to be 76.7 and 54.5 kJ/mol, respectively. As far as the authors know, no reference data related to these activation energies are available in the literature. The activation energy of the HNO_2 formation reaction is higher than that of any other reactions involved, implying that the rate determining step in the catalytic wet oxidation of ammonia would be the aqueous NH_3 oxidation reaction to HNO_2 which follows the third-order kinetics with respect to the catalytic sites of activated oxygen.

Table 2. Kinetic parameters estimated in the Arrhenius equation form

Constants	Pre-exponential factor	ΔH or E_A, kJ/mol	R^2
K_1 (bar^{-1})	1.649×10^{-5}	−20.7 (=ΔH)	0.80
k_2 (h^{-1})	1.362×10^{16}	123.1	0.98
k_3 (h^{-1})	6.697×10^{16}	86.5	0.99
k_4 (h^{-1})	2.448×10^{5}	61.1	0.91
k_5 (L mol^{-1} h^{-1})	7.106×10^{12}	76.7	0.95
k_6 (h^{-1})	3.133×10^{7}	54.5	0.99

Fig. 3 shows the parity plots for NH_3-N conversion, N_2 yield, and NO_3^- concentration. The predicted data are obtained using the parameter values in Table 2 for the oxidation reaction in the range of T=160-220 °C and P_{O_2}=4.8-11.1 bar for the 1,000 ppm NH_3 solution of $pH_{25,i}$=12.2. Predictions of NH_3-N conversion, N_2 yield, and NO_3 concentration are reasonably correspondent to the experimental data with the regression coefficients of 0.98, 0.96, and 0.73, and the standard deviation of residuals of 3.5, 3.5, and 84.4, respectively. Therefore, the kinetic model with the parameter values in Table 2 is thought to be properly established for the aqueous ammonia oxidation reaction.

Fig. 4 shows the simulated effects of the initial pH adjustment at 25 °C for the 1,000 ppm NH_3 solution on the performance of the oxidation reaction at T=215 °C and P_{O_2}=12 bar. This reaction condition was chosen for the influence of a small adjustment in the $pH_{25,i}$ to be highly exerted on the reaction performance under the

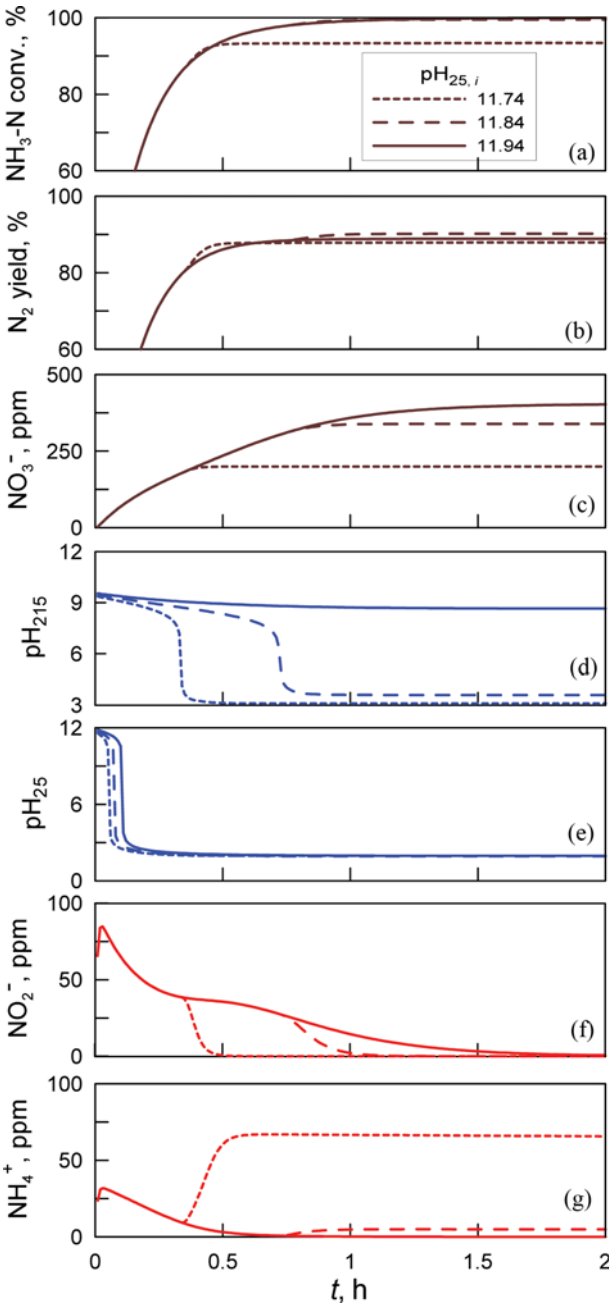

Fig. 4. Effects of the initial pH adjustment for the 1,000 ppm NH_3 solution on the performance of the oxidation reaction at T= 215 °C and P_{O_2}=12 bar ((a) NH_3-N conversion, (b) N_2 yield, (c) NO_3^- concentration, (d) pH at 215 °C, (e) pH at 25 °C, (f) NO_2^- concentration, and (g) NH_4^+ concentration).

situation where the reaction is terminated within 2 h of run. As shown in Fig. 4(a) and 4(c), the conversion of NH_3-N and the formation of NO_3^- are the highest for the solution of the highest $pH_{25,i}$=11.94, suggesting that both reactions are more facilitated for the solution of higher initial pH. However, as shown in Fig. 4(b), the N_2 yield is maximized when the $pH_{25,i}$ of the solution is adjusted to 11.84. This indicates that there is an optimum value of the $pH_{25,i}$ for promoting the oxidation conversion of ammonia to desirable N_2 instead of undesirable NO_3^-. Fig. 4(c) shows there could be considerable differences in the resulting NO_3^- concentrations depending on only a little difference in the $pH_{25,i}$ of the solution. The amount of hydroxyl ions present in the solution is increased to 1.26 times more if its pH is raised by 0.1. For the solution at higher pH as compared with that at lower pH, raising the pH by 0.1 means a greater increase in the amount of hydroxyl ions. The reason that the standard deviation of residuals for NO_3^- concentrations as relatively large as 84.4 in the parity plot of Fig. 3 could be attributed to some experimental errors in relation to the initial pH adjustment and measurement in the preparation for the ammonia solution of the pH as high as 12.2.

As shown in Fig. 4(d), for the solutions of $pH_{25,i}$=11.74 and 11.84, the equivalence points on the pH curve of the reacting solution at 215 °C are placed at the ammonia conversions of about 85.2% and 97.7%, respectively. After the occurrence of the equivalence point on the pH_{215} curve, drastic changes in the concentrations of NO_2^- and NH_4^+ species are followed in the reacting solutions at 215 °C, as shown in Fig. 4(f) and 4(g), respectively. However, there are no such sharp changes in the reaction for the solution of $pH_{25,i}$=11.94 because of no such equivalence point on the pH_{215} curve. Although the equivalence point is present on the pH_{25} curve, as shown in Fig. 4(e), it has no relation to the reaction behavior for the reacting solution at 215 °C. During the period of reaction before the equivalence point on the pH_{215} comes out, the reaction behavior for the solution of $pH_{25,i}$=11.74 or 11.84 follows the same locus as for the solution of $pH_{25,i}$=11.94. For the solution of $pH_{25,i}$=11.74, after the occurrence of the equivalence point at the ammonia conversions of about 85.2%, the reaction becomes actually terminated, giving the NH_3-N conversion of 93.4%, the N_2 yield of 87.9%, and the NO_3^- concentration of 199.6 ppm. On the equivalence point, alkaline water dominant aqueous NH_3 species is transformed to acidic water dominant NH_4^+, as shown in Fig. 4(g). N_2 formation by the reaction R5 is kinetically promoted with such increased concentration of NH_4^+, resulting in the rapid depletion of NO_2^- as well as a slight increase in the N_2 yield, as shown in Fig. 4(b) and 4(f). Because aqueous NH_3 species is not available any more in the reacting solution under acidic environment, no further oxidation reaction proceeds, leaving unreacted NH_3-N as NH_4^+ species in relatively high concentration, 66 ppm, as shown in Fig. 4(g).

It is therefore crucially important for the maximization of N_2 yield as well as the minimization of unreacted NH_3-N that the $pH_{25,i}$ of the solution should be adjusted for the acid-base equivalence point in the reacting solution at a reaction temperature to be placed at the ammonia conversion as high as possible. In this regard, the adjustment of $pH_{25,i}$=11.84 for the current 1,000 ppm NH_3 solution would be the best choice where the equivalence point on the pH_{215} curve is placed at the ammonia conversion as high as 97.7%, as shown in Fig. 4(a) and 4(d). For this case, the reaction becomes discontinued by the depletion of aqueous NH_3 to be oxidized, giving the NH_3-N conversion of 99.5%, the N_2 yield of 90.2%, the NO_3^- concentration of 339 ppm, and unreacted NH_3-N as NH_4^+ species of 5 ppm. For the solution of $pH_{25,i}$=11.94, having no equivalence point on the pH_{215} curve, as shown in Fig. 4(d), the reaction R2 proceeds continuously up to 2 h of run under the alkaline environment until the aqueous NH_3 species becomes depleted, giving the NH_3-N conversion of 99.9% and the N_2 yield of 88.9%.

In this situation, NO_2^- species formed from the on-going NH_3 oxidation reaction is relatively abundant as compared with the scarcity of NH_4^+ species, as shown in Fig. 4(f) and 4(g). Consequently, the reaction of N_2 formation is restricted, but that of NO_3^- formation proceeds continuously up to its concentration as high as 403 ppm, as shown in Fig. 4(b) and 4(c).

CONCLUSIONS

Reaction behavior of the catalytic wet air oxidation of 1,000 ppm aqueous NH_3 over Ru/TiO_2 catalyst could be successfully depicted through a kinetic model based on the reaction steps proposed. Kinetic parameters, such as the enthalpy of dissociative adsorption of O_2 onto the catalyst, or activation energy and pre-exponential factor in each reaction step, were optimally determined. The catalytic oxidation reaction of aqueous NH_3 to HNO_2 could be regarded as a rate-determining step by its highest activation energy of 123.1 kJ mol^{-1}. Throughout the simulation for the maximization of desirable N_2 yield against undesirable NO_3^- as well as the minimization of unreacted NH_3, it was found that the initial pH of the ammonia solution should be carefully adjusted for the acid-base equivalence point in the reacting solution at a reaction temperature to be placed at the NH_3 conversion as high as possible. For the 1,000 ppm NH_3 solution, such an optimum initial pH was simulated to be 11.84 by having the equivalence point in the reacting solution be placed at the ammonia conversion of about 97.7%. This simulated reaction at 215 °C under 12 bar of O_2 pressure became terminated by the depletion of aqueous NH_3 to be oxidized, giving the NH_3-N conversion, 99.5%; N_2 yield, 90.2%, NO_3^- concentration, 339 ppm; unreacted NH_3-N as NH_4^+ species, 5 ppm.

ACKNOWLEDGEMENT

This study was conducted by research funds from Gwangju University in 2016.

REFERENCES

1. L. Oliviero, J. Barbier Jr. and D. Duprez, *Appl. Catal. B: Environ.*, **40**, 163 (2003).
2. J. Qin and K. Aika, *Appl. Catal. B: Envrion.*, **16**, 261 (1998).
3. J. Taguchi and T. Okuhara, *Appl. Catal. A: Gen.*, 194-195, **89** (2000).
4. J. Barbier Jr., L. Oliviero, B. Renard and D. Duprez, *Catal. Today*, **75**, 29 (2002).
5. C.-M. Hung, J.-C. Lou and C.-H. Lin, *Chemosphere*, **52**, 989 (2003).
6. S. Kaewpuang-Ngam, K. Inazu, T. Kobayashi and K. Aika, *Water Res.*, **38**, 778 (2004).
7. C.-M. Hung, W.-B. Lin, C.-L. Ho, Y.-H. Shen and S.-Y. Hsia, *Water Environ. Res.*, **82**, 686 (2010).
8. V. Fontanier, S. Zalouk and S. Barbati, *J. Environ. Sci.*, **23**, 520 (2011).
9. F. Arena, R. D. Chio, B. Gumina, L. Spadaro and G. Trunfio, *Inorg. Chim. Acta*, **431**, 101 (2015).
10. C. Lousteau, M. Besson and C. Descorme, *Catal. Today*, **241**, 80 (2015).
11. J. Fu, K. Yang, C. Ma, N. Zhang, H. Gai, J. Zheng and B. H. Chen, *Appl. Catal. B: Envrion.*, **184**, 216 (2016).
12. R. Ukropec, B. F. M. Kuster, J. C. Schouten and R. A. van Santen, *Appl. Catal. B: Envrion.*, **23**, 45 (1999).
13. D. K. Lee, *Environ. Sci. Technol.*, **37**, 5745 (2003).
14. D. K. Lee, J. S. Cho and W. L. Yoon, *Chemosphere*, **61**, 573 (2005).
15. D. R. Lide, CRC Handbook of Chemistry and Physics, 73rd Ed., CRC Press, London (1993).
16. A. V. Bandura and S. N. Lvov, *J. Phys. Chem. Ref. Data*, **35**, 15 (2006).